uc3m | Universidad Carlos III de Madrid

e-Archivo

This is a postprint version of the following published document:

Hernández-Jiménez, F., Sánchez-Prieto, J., Cano-Pleite, E., Garcia-Gutierrez, L. & Acosta-Iborra, A. (2016). Development of an empirical wall-friction model for 2D simulations of pseudo-2D bubbling fluidized beds. *Advanced Powder Technology*, 27(2), pp. 521-530.

DOI: 10.1016/j.apt.2016.02.001

© 2016 The Society of Powder Technology Japan.

This work is licensed under a Creative Commons Attribution-NonCommercial-NoDerivatives 4.0 International License.

Development of an empirical wall-friction model for 2D simulations of pseudo-2D bubbling fluidized beds

F. Hernández-Jiménez[a,*], J. Sánchez-Prieto[a], E. Cano-Pleite[a], L. M. Garcia-Gutierrez[a], A. Acosta-Iborra[a]

[a] *Universidad Carlos III of Madrid, Department of Thermal and Fluid Engineering. Av. de la Universidad 30, 28911, Leganés, Madrid, Spain*

Abstract

Pseudo−2D fluidized beds have been crucial for the understanding of the dynamics of gas−particle systems. In these systems the distance between the front and back walls is narrow, which restricts and creates a resistance to the solids motion, leading to a different flow behaviour compared to fully 3D systems. This interaction of the particle motion with the walls can be significant and should not be neglected in numerical simulations. The present work develops a new model to easily account for the friction effect between the walls and the particles in a pseudo−2D bed. The model is based on experimental results combined with simplifications of the shear force on a wall provided by the kinetic theory of granular flows. The dependence on the particle diameter and bed thickness is directly introduced in the model through the use of a straightforward expression that is easy to code and does not lead to numerical divergence. To test the model two beds of different thickness were simulated, and the resulting time-averaged solids concentration and velocity as well as bubble properties were compared with experiments. It is shown that the numerical results with the new wall-friction model improve the prediction of the standard 2D−simulations.

Keywords: Fluidized bed, Pseudo-2D, Wall friction, CFD

1. Introduction

Fluidized beds have several applications in chemical and process industries, such as fluid catalytic cracking (FCC), gasification, combustion of solid fuels, Fischer−Tropsch synthesis, drying and coating [1]. Despite the fact that fluidized beds have been used for these processes since the 1920s and great progress has been made, some aspects of fluidized bed dynamics are still far from being fully understood and, hence, they constitute active fields of research. These aspects include, for example, general bed dynamics, gas interaction with particles, particle mixing, bubble formation, behaviour of fuel particles in fluidized bed reactors, segregation, agglomeration, vibrofluidization and scaling-up of the bed behaviour [2, 3, 4, 5, 6, 7, 8, 9]. Therefore, there is a need of experimentation and modelling of fluidized beds. In this regard, pseudo−two−dimensional

*Corresponding author. Tel:+34 91 624 8344
Email address: fhjimene@ing.uc3m.es (F. Hernández-Jiménez)

(pseudo−2D) beds, which are lab−scale beds of simplified geometry, have been crucial for the understanding of the dynamics of gas−particle systems. Pseudo−2D fluidized bed systems typically have a transparent front wall in order to allow optical access to the system. The back wall of the bed is separated to the front wall by a narrow distance to ensure that the visualization is representative of the whole system. Thus, the bed volume enclosed between the front and back walls has a small thickness.

Numerical simulations, either using Eulerian−Eulerian two-fluid models (TFM) [10, 11, 12], Eulerian−Lagrangian approaches, such as discrete element models (CFD-DEM) [13, 14], or a combination of both strategies [15], can be a very effective complementary tool to experiments for achieving a detailed analysis of the hydrodynamics of complex gas−solids flows [16, 17]. The CFD-DEM strategy is based on a Lagrangian simulation of each particle trajectory coupled with an Eulerian simulation of the bulk gas flow. The gas-solid interaction is computed through semi-empirical closure models to reduce the level of detail required in the solution of the gas phase. In the TFM approach, the gas phase and the particles or solids phase are treated as two interpenetrating and continuum media in an Eulerian framework using the conservation equations of fluids. As in the case of the Eulerian-Lagrangian approach, the two-fluid simulation of fluidized beds requires the use of closure models for the gas-solids interaction, but also constitutive closures are needed for the solid stress which are usually based on the granular kinetic theory [11] through the concept of granular temperature, accounting for the random fluctuations of particles' velocity. CFD-DEM simulations have a larger computational cost because they solve the individual motion of each particle and the collisions between them. As a consequence, CFD-DEM simulations can reproduce the micro−scale of the bed concerning the particles' dynamics provided the number of particles is not very large (i.e. typically small−sized beds). Finally, the most detailed Eulerian−Lagrangian simulation strategy for fluidized beds is the direct numerical simulation (DNS) of the fluid flow surrounding solid particles together with the Lagrangian description of the particles' interaction. In the DNS approach, lattice Boltzmann methods are normally used (see for example, [18, 3]), although finite volume schemes are also employed [19]. The direct simulation of gas−fluidized beds is quite attractive since all the bed physics can be reproduced from first principles. However huge computational resources are required, restricting DNS simulations to beds with a relatively small number of particles. Therefore TFM simulations are currently the most suitable strategy for the simulation of both the macro− and meso−scales of the bed when the number of particles involved is high. This allows for the simulation of medium and moderately−large sized beds commonly used in laboratory research and pilot plant testing. For this, reliable submodels are required for incorporating in TFM the micro-scale of the interactions between gas, particles and walls of the bed.

In pseudo−2D beds the front and the back walls restrict and create resistance on the solids motion, leading to a different flow behaviour compared to fully three−dimensional (3D) systems [20, 21]. For beds of small thickness, the effect of the front and the back walls on the particle motion can be significant and should not be neglected in numerical simulations of pseudo−2D beds, as initially reported by Li et al.

[22] and Hernández-Jiménez et al. [23]. Moreover, the wall effect in numerical simulations of gas−solids pseudo−2D systems has been investigated in several numerical studies using either TFM or CFD-DEM [24, 25, 22, 26]. These studies recommended the use of 3D simulations instead of 2D in order to get a more accurate prediction of pseudo-2D gas−solid fluidized beds, i.e. the wall effect must be included in the simulations. However, 3D simulations require much more computational resources than 2D simulations.

Recently, Li and Zhang [21] implemented a model for 2D simulations to account for the front and back wall effects in a pseudo-2D gas−solid fluidized bed without the need of a 3D simulation. Their model relied mainly on the kinetic theory of granular flows applied to shear forces and granular temperature balances on the wall. The equations of these balances assume isotropy and simple shear in the granular flow. Li and Zhang [21] introduced the shear force imposed by the front and back walls as a body force acting on the solids flow and a source term in the granular temperature equation. They assumed that collisions between particles and walls are of sliding type. Maps of concentration of solids fraction and profiles of vertical velocity of the solids phase were analysed by Li and Zhang [21] and the velocity profiles were compared with reported experimental results. They obtained results with their 2D modified model that improved those obtained when the system is modelled just as 2D, and the computational cost was greatly reduced compared with a 3D simulation. Also, very little differences were found between considering or not the source term accounting for the effect of the front and back walls in the granular temperature equation.

Besides, the front and back walls effect on the solids motion were characterised in [20, 27] using a novel experimental technique and with CFD-DEM simulations. Hernández-Jiménez et al. [20] experimentally investigated the overall frictional force due to the walls on the solid particles by linking the digital images acquired in a pseudo-2D bed with the pressure measurements. They proposed a force balance in order to estimate this frictional force and characterised it using a particle−wall interaction coefficient, c. Hernández-Jiménez et al. [27] verified this interaction coefficient with CFD-DEM simulations and performed a local study of the wall−particle frictional forces. It was found that the local value of the coefficient c in the CFD-DEM simulations is similar to the global value experimentally obtained.

The objective of the present study is to develop an empirical model to easily account for the particle-wall interaction effect in pseudo−2D bubbling fluidized beds to outperform the limitations of common 2D and 3D approaches indicated previously. In particular, the model allows for the wall−friction simulation of pseudo−2D beds using a 2D domain instead of a more computationally demanding 3D domain. The complex particle-wall interaction given by the kinetic theory of granular flows is simplified as a function of the velocity of the particles in the pseudo−2D bed, as suggested by Hernández-Jiménez et al. [20, 27]. Then, a general expression for the particle−wall interaction is developed by combining dimensional analysis and the experimental observations by Hernández-Jiménez et al. [20]. The result is an empirical wall−friction model that is implemented in a two−fluid model using the methodology described by Li and Zhang [21]. The relevance of the proposed wall−friction model is that direct experimental evidence about the particle−wall

interaction in pseudo−2D beds is used to improve the prediction of the numerical simulations. In contrast to Li and Zhang's model, the present model introduces the dependence of the particle−wall friction as a function of the particle diameter and bed thickness through the use of a very simple expression instead of using a complex function of the granular temperature.

Two different pseudo−2D fluidized beds are simulated to check the consistency of the model proposed. The first pseudo−2D bed is the experimental set-up employed by Hernández-Jiménez et al. [20] to characterise the particle-wall interaction effect. The second bed is the system experimentally studied by Laverman et al. [28]. The simulation results of these two fluidized beds are compared with their corresponding experimental data. The present study performs a practical validation of the model with experiments for a complete range of important parameters for the bed operation: the solids concentration maps, the vertical velocity of solids at different heights, the gulf stream circulation of solids and the bubble behaviour in the bed. The results will show that the incorporation of the wall-friction model produces a clear improvement of the standard 2D simulations.

2. Theory

Resorting to the kinetic theory of granular flows, Johnson and Jackson [29] proposed the following force balance for the boundary condition to solve the motion of a granular material on an infinite horizontal plate.

$$\frac{\vec{v}_{sl}}{|\vec{v}_{sl}|} \cdot (\overline{\overline{\sigma_c}} + \overline{\overline{\sigma_f}}) \cdot \vec{n} + \frac{\Phi\sqrt{3\Theta}\rho_s\alpha_s g_0|\vec{v}_{sl}|}{6\alpha_{s,max}} + N_f \tan\phi = 0 \tag{1}$$

here, $\vec{v}_{sl}$ is the slip velocity between the particles and the plate, $\overline{\overline{\sigma_c}}$ and $\overline{\overline{\sigma_f}}$ are the collisional-translational and frictional contributions to the stress tensor, respectively, $\vec{n}$ is the unit normal from the boundary into the particle assembly, Φ is a specularity coefficient with values between zero for perfectly specular collisions and unity for perfectly diffuse collisions, Θ is the granular temperature, ρ_s is the solids density, α_s is the solids volume fraction, g_0 is the radial distribution function at contact, $\alpha_{s,max}$ is the solids concentration at closest random packing, N_f represents the normal contribution to the shear stress and ϕ is the angle of internal friction.

The first term at the left hand side of Equation 1 represents minus the bulk shear stress in the direction of the slip velocity, $-\tau_{bc}$, the second term accounts for the collisional contribution to the shear force and the third term to the Coulomb's friction contribution due to the material sliding over the surface. Therefore, Coulomb's friction and collision must compensate the bulk shear stress at the wall. In the present study, th e hear force produced by the two contributions describe above will be denoted, for brevity, as "wall−friction". Both friction and collision depends on several parameters related to the physical properties of the granular material, the solids fraction, the shear force normal to the wall, the granular temperature and the velocity of the particles. However, the closure models describing Θ, N_f and g_0 to calculate τ_{bc} from Equation 1 can be

quite complex and their application to pseudo−2D beds is still an open question. Nevertheless, the granular temperature, Θ (i.e. solids velocity fluctuations), is mainly generated at the wall by the difference between the velocity of the solids and the wall, $\vec{v}_{sl}$. Besides, the normal shear force, N_f, is a function of the granular temperature. Therefore, τ_{bc} inEquation 1 is a strong function of the slip velocity in parallel to the wall and can be linearised, as a first approximation, as:

$$\tau_{bc} = a|\vec{v}_{sl}| + b \tag{2}$$

where a and b are linearisation constants that depend on the physical and geometrical properties of the granular material. It is worth to mention that Johnson and Jackson [29] developed their theory for the shearing region associated to a single horizontal plate of an isotropic granular flow. This situation is certainly different to what occurs between the two vertical walls of a pseudo−2D bed. In this case the front and back walls affect simultaneously the granular flow since they are very close to each other. Therefore, given the approximate character of Equation 1 when applied to a pseudo−2D bed, only the dependence of τ_{bc} on the slip velocity will be retained, as indicated in Equation 2. Then, the relative importance of the two terms in Equation 2 when applied to a pseudo−2D bed should be evaluated, which is not a trivial task.

Firstly, Hernández-Jiménez et al. [20] experimentally estimated the overall frictional force between the solids and the front and back walls of a pseudo−2D bed. They found a linear dependence of such forces with the solids bulk velocity for the operative conditions analysed. In a second study, Hernández-Jiménez et al. [27] numerically analysed the same system by means of CFD-DEM simulations and found that the numerical results also predict a linear dependence of the frictional forces with the velocity of each individual particle. Inspection of these numerical results indicate that in fact $a|\vec{v}_{sl}|$ is typically greater than b. Finally, the above studies are conceptually supported by the fact that in a real fluid between narrow walls the frictional forces are proportional to the velocity. In a real fluid, the pressure drop ΔP, when the fluid is moving through a channel is given by:

$$\Delta P = \frac{1}{2} v^2 \rho_s \frac{L}{D_h} f \tag{3}$$

where f is the friction coefficient, L is the length of the duct and D_h is the hydraulic diameter. In laminar flows and beginning of turbulence (i.e. not very high velocities or very viscous flows), f is inversely proportional to the Reynolds number, therefore, $f \sim A/v$. Thus:

$$\Delta P \sim \frac{1}{2} v^2 \rho_s \frac{L}{D_h} \frac{A}{v} \sim Bv \tag{4}$$

where A and B are constants.

As the pressure drop is proportional to the shear stress of the wall, Equation 4 indicates that the shear

stress in a fluid flowing in a duct, or between two close parallel walls, is proportional to the velocity. This can be considered true as a first approximation for the solids in a fluidized bed given their fluid like behaviour. Therefore, comparing Equations 2 and 4 and taking into account the aforementioned works, the constant b in Equation 2 will be neglected compared to the term $a|\vec{v}_{sl}|$ for the specific range and conditions analysed in the present study (pseudo-2D bed of restricted thickness working in bubbling regime), so the shear force will be considered just proportional to the solids velocity. In the following lines dimensional analysis is applied to estimate the parameter a in Equation 2.

It was experimentally shown by Hernández-Jiménez et al. [20] that the global wall friction force on the particles can be calculated as $F_{fric} = cA_L dy_{cm}/dt$, which depends on a global particle-wall interaction coefficient, c, the surface area of the two lateral walls in contact with the bed, A_L, and the velocity of the centre of mass, dy_{cm}/dt. Hernández-Jiménez et al. [20] also found that the global particle-wall interaction coefficient c, mainly depends on the particle diameter, and the following quadratic function was fitted to reproduce the variation of the coefficient, c, with the particle diameter, d_s:

$$c = c_1 d_s^2 + c_2 \tag{5}$$

where c_1 and c_2 are constants with the following values: $c_1 = 4.86 \cdot 10^7$ [kg/m^{4}s] and $c_1 = 43.8$ [kg/m^{2}s].

These experimental results were obtained for a pseudo-2D bed of thickness $Z = 1$ cm, which means that the proposed correlation may be valid only for beds of such thickness. Therefore, a dimensional analysis can be performed to predict how the effect of the bed thickness could be included in Equation 5. Generally speaking, the particle-wall interaction coefficient, c, (global or local) is a function of the particle diameter, d_s, the solids density, ρ_s, the relative gas velocity, U/U_{mf}, the thickness of the bed, Z, the static bed height, h_0, the width of the bed, W, the gravity, g, the gas density, ρ_g, the Coulomb's friction coefficient, μ, and other parameters related to the geometrical and elasticity characteristics of the particles (e.g. maximum packing limit, sphericity, rugosity and restitution coefficient of the particles).

$$c = f(d_s, \rho_s, \rho_g, U/U_{mf}, Z, H, W, g, \mu, \text{geometry-elasticity}) \tag{6}$$

Using the Buckingham Π theorem, the dimensionless particle-wall interaction coefficient can be expressed as follows:

$$\frac{c}{\rho_s Z^{1/2} g^{1/2}} = f'\left(\frac{d_s}{Z}, \frac{U}{U_{mf}}, \frac{\rho_g}{\rho_s}, \frac{h_o}{W}, \frac{W}{Z}, \mu, \text{geometry-elasticity}\right) \tag{7}$$

Hernández-Jiménez et al. [20] experimentally demonstrated that the global particle-wall interaction coefficient is basically a function of d_s, μ and the geometrical and elasticity characteristic of the particles, therefore:

$$\frac{c}{\rho_s Z^{1/2} g^{1/2}} = f''\left(\frac{d_s}{Z}, \mu, \text{geometry-elasticity}\right) \tag{8}$$

Note that Equation 5 was obtained for the conditions $Z = 1$ cm, $g = 9.81$ m/s^2 and $\rho_s = 2500$ kg/m^3. Thus, comparing Equation 5 with Equation 8 the following dependence of the particle-wall interaction coefficient on the thickness Z arises:

$$\frac{c}{\rho_s Z^{1/2} g^{1/2}} = 6.2\left(\frac{d_s}{Z}\right)^2 + 5.6 \cdot 10^{-2} \tag{9}$$

All the variables in Equation 9 are expressed in SI units. Finally, Equation 9 suggests that the particle-wall interaction coefficient increases when the thickness of the bed tends to small values for a given value of particle diameter, since:

$$c = 6.2\frac{d_s^2 \rho_s g^{1/2}}{Z^{3/2}} + 5.6 \cdot 10^{-2} \rho_s Z^{1/2} g^{1/2} \tag{10}$$

Note that Equation 10 also shows that c increases again for large values of Z. Nevertheless, this behaviour is an artifact caused by the quadratic function used to fit the experimental data and weakly affects the value of c if the ratio d_s/Z is small.

In a subsequent study, Hernández-Jiménez et al. [27] demonstrated by means of CFD-DEM simulations that the value of the local coefficient c in the CFD-DEM simulations is similar to the global value experimentally obtained. Therefore, the frictional force calculated as $\vec{F}_{fric,loc} = cA_{loc}\vec{v_s}$ can be locally applied to a small portion of solid phase affected by a given local surface area A_{loc}, with $\vec{v_s}$ as the local solids velocity of that small portion. For example, if a two-fluid model simulation is solved in 2D dimensions, $\vec{F}_{fric,loc}$ can be incorporated as an extra body force in the momentum equation balance for the solids phase. This procedure will be described in the following subsection.

It is important to highlight that the model developed in this work stands out for its simplicity that considers explicitly the most important variables, which are the particle diameter and the bed thickness, without the need of including more complex variables that will make the code to slow down or even to diverge.

2.1. Numerical model

The open-source MFIX-TFM code, developed at US Department of Energy's National Energy Technology Laboratory, was used to conduct the numerical simulations. In the MFIX-TFM code, an Eulerian-Eulerian two-fluid model approach is proposed. The continuum description of the gas and dense phases (i.e. two-fluid model) is based on the conservation equations of mass, momentum and granular temperature [30, 31]. The kinetic theory of granular flow, which characterizes the stochastic fluctuations of the solids kinetic energy,

was used for the closure of the solids stress terms. The closure expressions for the Eulerian-Eulerian model can be found in [31].

The governing equations of the two-fluid model, applied to a 2D domain representing a vertical section of the pseudo−2D bed, are summarised in the following lines.

Mass conservation of the gas (g) and solid (s) phases:

$$\frac{\partial}{\partial t}(\alpha_g \rho_g) + \nabla \cdot (\alpha_g \rho_g \vec{v_g}) = 0 \tag{11}$$

$$\frac{\partial}{\partial t}(\alpha_s \rho_s) + \nabla \cdot (\alpha_s \rho_s \vec{v_s}) = 0 \tag{12}$$

Momentum conservation of the gas phase:

$$\begin{aligned} \frac{\partial}{\partial t}(\alpha_g \rho_g \vec{v_g}) + \nabla \cdot (\alpha_g \rho_g \vec{v_g} \vec{v_g}) = \\ -\alpha_g \nabla p + \nabla \cdot \overline{\overline{\tau_g}} + \alpha_g \rho_g \vec{g} - K_{gs}(\vec{v_g} - \vec{v_s}) \end{aligned} \tag{13}$$

Momentum conservation of the solid phase:

$$\begin{aligned} \frac{\partial}{\partial t}(\alpha_s \rho_s \vec{v_s}) + \nabla \cdot (\alpha_s \rho_s \vec{v_s} \vec{v_s}) = \\ -\alpha_s \nabla p - \nabla p_s + \nabla \cdot \overline{\overline{\tau_s}} + \alpha_s \rho_s \vec{g} - \vec{f}_{fric} + K_{gs}(\vec{v_g} - \vec{v_s}) \end{aligned} \tag{14}$$

where p_s is the solids pressure, $\overline{\overline{\tau_i}} = \alpha_i \mu_i (\nabla \vec{v_i} + \nabla \vec{v_i}^T) + \alpha_i (\lambda_i - \frac{2}{3}\mu_i) \nabla \cdot \vec{v_i} \overline{\overline{I}}$ is the stress tensor for phase i.

As can be seen in Equation 14, the extra term $\vec{f}_{fric}$ is incorporated to account for the effect of the front and back walls of the pseudo-2D bed in an analogous way to [21] but using Equation 2. This extra term has been neglected for the gas phase as it is expected to have a comparatively minor effect. The terms in the right hand side of Equation 14 are forces per unit volume. Thus, to incorporate the effect of the front and back walls on the particle momentum balance, the local friction forces exerted by the front wall on a portion of surface area, A_{loc}, and by the opposite back wall on a similar value of A_{loc}, should be divided by the volume contained within these two local portions of walls:

$$\vec{f}_{fric} = \frac{\vec{F}_{fric,front} + \vec{F}_{fric,back}}{A_{loc} Z} \tag{15}$$

where Z is the thickness of the bed. Therefore the extra body force term accounting for the friction of the front and back walls per unit volume in the bed is:

$$\vec{f}_{fric} = \frac{2cA_{loc}\vec{v_s}}{A_{loc}Z} = \frac{2c\vec{v_s}}{Z} \tag{16}$$

Equation 16 assumes that the solids velocity vector, $\vec{v_s}$, is approximately similar in the front and back walls and equal to the central plane vector velocity in a pseudo-2D bed. Equation 10 is used to calculate the coefficient c in Equation 16.

Finally, the balance for the granular temperature, Θ, is:

$$\begin{gathered} \frac{3}{2}\left(\frac{\partial}{\partial t}(\rho_s\alpha_s\Theta) + \nabla\cdot(\rho_s\alpha_s\vec{v_s}\Theta)\right) = \\ (-p_s\overline{\overline{I}} + \overline{\overline{\tau_s}}) : \nabla\vec{v_s} + \nabla\cdot(k_\Theta\nabla\Theta) - \gamma_\Theta - 3K_{gs}\Theta \end{gathered} \tag{17}$$

where $(-p_s\overline{\overline{I}} + \overline{\overline{\tau_s}} : \nabla\vec{v_s})$ is the generation of Θ by the solids stresses, $k_\Theta\nabla\Theta$ is the diffusion of Θ, γ_Θ is the collisional dissipation of Θ and $3K_{gs}\Theta$ is the transfer of random kinetic energy between the solids and the gas. In Equations 13, 14 and 17, K_{gs} is the drag force between the gas and the solid phase. For simpliciy, the effect of the front and back walls on the net production of granular temperature in the bed will not be considered here, as it has been proven to have a negligible effect on the velocity profiles [21]. The drag force correlation for the gas-solid interaction used in this work is the one proposed by Gidaspow [11].

3. Experimental and simulated systems

Two different pseudo-2D bed configurations were chosen to carry out the simulations and to compare the obtained results with experimental data. The first configuration (Configuration 1) is the bed employed by Hernández-Jiménez et al. [20] to characterize the particle-wall interaction coefficient, c, by means of Digital Image Analysis (DIA). The second configuration (Configuration 2) is the bed studied by Laverman et al. [28] to analyse the hydrodynamics of pseudo-2D beds using Particle Image Velocimetry (PIV). The beds studied in Hernández-Jiménez et al. [20] and in Laverman et al. [28] have been selected because the two experiments are different in important parameters such as the bed thickness, the particle diameter and the superficial gas velocity. Table 1 summarises the main parameters of these bed configurations. Particle density in the system tested by Laverman et al. [28] was assumed to be 2500 kg/m^3 as the particles were ballotini glass beads.

In the experimental bed corresponding to Configuration 1, DIA was applied to distinguish between bubble (B) and dense phase (C). The images were recorded with a digital camera Basler A640, which took images of the front view of the fluidized bed at 100 frames per second. In addition to DIA, PIV was applied to obtain the velocity of the particles in the present study. To enhance the cross-correlation in the PIV calculation, a small fraction of bed material was painted in black. This allowed the calculation of bubble size and velocity as in the experiment of Laverman et al. [28] for Configuration 2. The dense phase velocity was

Table 1: Main parameters of the experimental fluidized beds simulated.

Pseudo-2D bed	**Configuration 1**	**Configuration 2**
Bed height, H (m)	1	0.7
Bed width, W (m)	0.3	0.3
Bed thickness, Z (m)	0.01	0.015
Static bed height, h_0 (m)	0.3	0.3
Particles density, ρ_s (kg/m^3)	2500	2500 (assumed)
Particle diameter, d_s (mm)	0.6-0.8	0.4-0.6
Minimum fluidization velocity, U_{mf} (m/s)	0.44	0.18
Dimensionless gas velocity, U/U_{mf} $(-)$	2	2.5

obtained using the multigrid PIV code MATPIV [32] with final interrogation windows of 16x16 pixels and 50% overlapping. Also following the procedure of Laverman et al. [28], the time-averaged velocity in both the experiment and the simulation was weighted with the spatial distribution of dense phase to correctly account for the influence of particle raining from the roof of the bubbles on the time-averaged particle velocity.

Regarding the numerical simulation of Configurations 1 and 2, a second order accurate scheme was selected to discretise the convective derivatives of the governing equations. In the two configurations, the 2D computational domain was meshed using square cells of length 5 mm for both systems, in accordance with Li et al. [22] and Hernández-Jiménez et al. [23]. The distributor was modelled as a uniform velocity inlet and a fixed pressure boundary condition was chosen at the top of the freeboard. The lateral walls of the bed were modelled as no-slip boundary condition for the gas and solid phases. It has been shown that the lateral boundary condition does not have a strong effect in this kind of simulations [22, 23]. The particle diameter used to model the dense phase in the simulations was equal to the average particle diameter in the corresponding experiment. The angle of internal friction was set to $\phi = 30$ deg, which is related to the Coulomb's coefficient of friction through $\tan\phi = \mu$. The interparticle coefficient of restitution was $e_s = 0.9$, the gas density $\rho_g = 1.2$ kg/m^3 and the gas viscosity $\mu_g = 1.8{\cdot}10^{-5}$ Pa·s. It is important to mention that the inclusion of the wall-friction term does not affect the speed of the simulations nor creates divergence problems compared to standard 2D simulations. The total time simulated was 60 seconds and the first 5 seconds of the start-up were removed to construct the time-averaged values.

4. Results

4.1. Configuration 1

The first part of the results focuses on comparing the PIV and DIA results obtained for experimetns in Configuration 1 with numerical results obtained from the two-fluid model simulations, with and without the

incorporation of the wall−friction term in the two-fluid model equations.

Figure 1 shows the dense phase probability, C, of the experimental case (Figure 1a) and the time-averaged solids volume fraction, α_s, in the 2D domain of the simulation (Figure 1b and 1c). The dense phase probability is calculated as the time-averaged value of the dense phase magnitude, which is 1 outside bubbles and 0 inside bubbles or in the freeboard. Hernández-Jiménez et al. [23] demonstrated that the dense phase probability, C, in the experimental data was analogous to the time-averaged solids volume fraction, α_s, obtained from the simulations. The time-averaged solids velocity vectors, $\vec{V}$, calculated from the PIV data in the experiment and from the dense phase velocity in the simulations, are also included in Figure 1. Note that the velocity vectors in Figure 1 are not plotted in the same scale for all the cases since their magnitude in the experiments is smaller than in the simulations when the later do not include the wall-friction term. Figure 1a shows that in the experiments there is a clear preferential path of bubbles towards the centre of the bed with a downflow of particles close to the lateral walls. Therefore, two recirculation regions centred at 0.15 m over the distributor are formed. Looking at the 2D simulations results in Figure 1b obtained without the front and back wall friction effects (standard 2D simulation), the differences with experiments are noticeable. The bubble path in Figure 1b is wider in the upper part of the bed than in the experiments. This is due to a more vigorous bubbling regime appearing in the simulations when the effect of front and back walls friction is not included. For the same reason, the centre of the recirculation region in the simulation results shown in Figure 1b is located at a lower height than in the experimental results of Figure 1a.

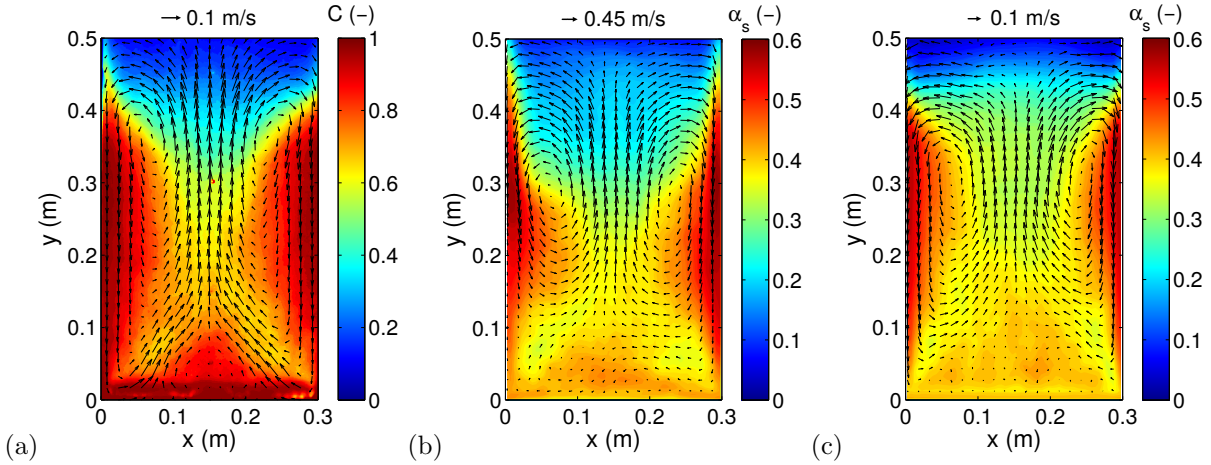

Figure 1: Experimental time-averaged dense phase probability overlaid with the time-averaged velocity vectors obtained with PIV (a), numerical time-averaged solids volume fraction overlaid with the time-averaged velocity vectors without the wall-friction term (b) and including it (c) in the solids momentum equation. Configuration 1.

Turning now to the 2D simulation that incorporates the term (Equation 16) accounting for the friction of the front and back walls on the bed material, it can be observed in Figure 1c that the mean solids fraction and

the recirculation of solids in the simulated bed are in this case much closer to the experimental observations (Figure 1a). The centre of the recirculations of solids in Figure 1c is placed close to the recirculations obtained in the experiments, Figure 1a. Close to the distributor, some differences can be appreciated in the solids volume fraction obtained with the simulations. This can be attributed to 3D effects in the experimental results caused by small bubbles, which are expected in that region. Most of these bubbles are not recorded because their diameter is smaller than the bed thickness. In contrast, all the bubbles in the simulations can be distinguished in spite of their size, because the numerical domain is purely 2D.

Figure 2 shows the solids hold up from the simulations and the experiments as a function of the distance to the distributor. In the figure the results are time averaged and spatially averaged over the horizontal direction along the whole bed width. In the simulations the solids hold up is directly obtained from the solids volume fraction. In the experiments, the distribution of solids is given by the dense phase probability. Figure 2 shows that, when the particle−wall friction term is included in the simulation, the resulting solids hold up has the same trend as the experiment. Up to 0.35 m over the distributor, an approximately constant value of the solids hold-up is observed, followed by a rapid decrease from about 0.35 m to 0.55 m. In contrast, according to Figure 2, the simulation without the particle-wall friction term yields a decrease of solids volume fraction that is more progressive than in the experiments and starts at a lower height (0.25 m approximately). This suggests that 2D simulations without the friction term tend to produce more vigorous bubble eruptions than real pseudo-2D beds.

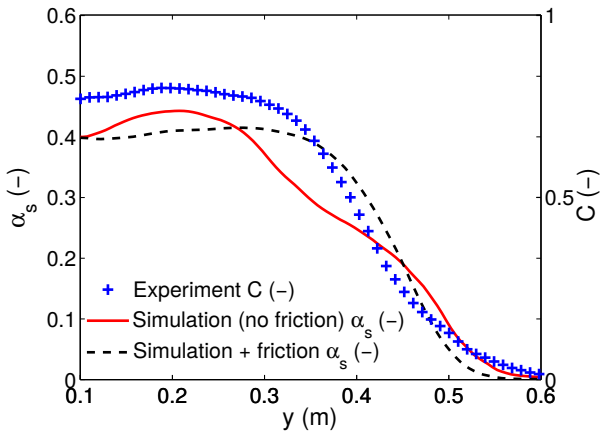

Figure 2: Solids hold up versus distance to the distributor, y. The experimental results correspond to the dense phase probability, C, whereas the solids volume fraction, α_s, is used in the simulation results.

Some advantages in the prediction of the solids and bubble flow patterns when the 2D simulation incorporates the effect of the front and back wall have been qualitatively shown in Figure 1. From a quantitative point of view, the main improvement comes with the prediction of the time-averaged solids velocity, whose principal component is the vertical velocity, V_y. Figure 3 shows the time-averaged vertical solids velocity,

V_y, versus the horizontal coordinate, x, at different heights, y, for the bed corresponding to Configuration 1. The figure comprises results from experiments and from 2D simulations with and without incorporating the term that accounts for the front and back wall friction. In Figure 3 it can be clearly seen an improvement in the prediction of both the velocity distribution and the velocity magnitude of the profiles when the wall−friction term is included in the simulations. In particular, the major improvement can be found in the velocity profile for the height of $y = 0.25$ m (Figure 3b), where a standard simulation without the wall−friction term clearly over-estimates the solids velocity magnitude. However, including the wall-friction term makes the simulation results practically equal to the experiments. This trend is not as marked for the lower height (Figure 3a) just because the solids flow is more uniformly distributed in the region close to the distributor, as can be also seen in Figure 1. Close to the distributor the solids velocity is less intense and the amount of data required to estimate mean values is higher. This explains the non-symmetrical profile of the solids vertical velocity at $y = 0.1$ m. Paying attention to the region close to the lateral walls, some differences between the simulation with the wall-friction term and the experiments can be appreciated. In this region the simulation results present a more pronounced descending flow compared to the experimental data. This discrepancy can be attributed to the modelling of the distributor plate, which consists of a perforated plate in the experimental system but it is modelled as a uniform velocity inlet in the simulations. Mesh limitations make difficult to discretise the orifices of the experimental distributor and the uniform velocity inlet chosen for the boundary condition is generally accepted as a good approximation. In the simulated distributor, since the gas is entering equally along the width of the bed, bubbles are created uniformly and this confines the descending area for the solids to a region very close to the wall, which increases the velocity magnitude of downward velocity of the solids in this region. The huge over-prediction of the solids velocity in a standard 2D simulation when the front and back walls friction effect is not included is in harmony with previous studies [22, 23]. Therefore, it can be seen that the inclusion of the wall-friction term clearly improves the prediction of the solids velocity magnitude. An analogous improvement was also reported by Li and Zhang [21].

The bubble behaviour is another feature of great interest when studying fluidized bed systems. Figure 4a shows the mean and standard deviation, σ, of the bubble diameter, D_b, as a function of the vertical distance to the distributor, y. Figure 4b contains the bubble vertical velocity, V_b, as a function of its diameter, D_b. Bubbles in the simulation results were identified by applying a threshold to the instantaneous solids volume fraction. Experimental and simulated bubbles are identified similarly applying a threshold to the gray scale level of the digital images acquired [33] and a threshold in the solids volume fraction for the simulation. This threshold in the simulations was chosen to be $\alpha_{s,th} = 0.3$, which leads to a definition of the bubble contour close to the one obtained with the thresholding in the experiments [23]. Both the mean and the standard deviation values presented in Figure 4 are calculated with the instantaneous values contained in each data interval in which the horizontal axis is divided. The results are presented for the experimental conditions

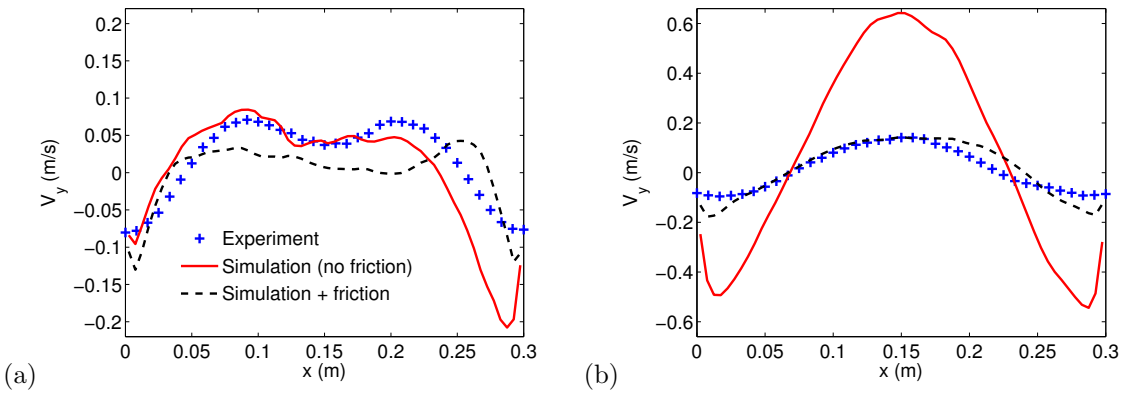

Figure 3: Time-averaged vertical solids velocity versus the horizontal coordinate, x, for the experimental results and the numerical prediction with and without considering the wall-friction term. Results are presented at two distances to the distributor: a) $y = 0.1$ m, and b) $y = 0.25$ m. Configuration 1.

as well as for the 2D simulation results with and without the term for the front and back walls friction (Equation 15). The incorporation of the friction term, $\vec{f}_{fric}$, tends to improve both the mean values and the standard deviation of the bubble characteristics obtained by the 2D simulations. In the case of the curves for mean and standard deviation of velocity versus the diameter of bubbles, Figure 4c and 4d, the impact of the wall-friction term in the simulation results is not as marked as for the case of bubble growth analysed in Figure 4a and 4b. This suggests that solids friction with front and back walls have greater influence in the growth of bubble diameter than in the coupling of diameter and velocity induced by gravity. The biggest discrepancy between the experiments and the 2D simulation with the wall−friction term seems to appear in the mean bubble diameter at a height around 0.2-0.25 m, which may be attributed to differences in capturing bubbles in the splash region of the simulated and experimental beds. Experimental bubbles were not completely captured in the splash region because the number of particles on its contour was reduced.

4.2. Configuration 2

The system studied in this section corresponds to the system used by Laverman et al. [28] (Configuration 2). It should be noted that the friction coefficient, c, to be used in Equation 15 was originally estimated with a bed similar to Configuration 1, whose thickness and operative conditions are different to Configuration 2. Thus, this section will clarify whether the improvements observed in the simulation of Configuration 1 are extensive to other pseudo-2D beds. An improvement when considering the wall−friction term has been shown for the results of Configuration 1. Results showing the over−prediction of the standard 2D configuration without this term are not included here to avoid repetitiveness with Section 4.1. Therefore, this subsection only focuses in the comparison of the experimental results with the simulation considering the wall−friction term.

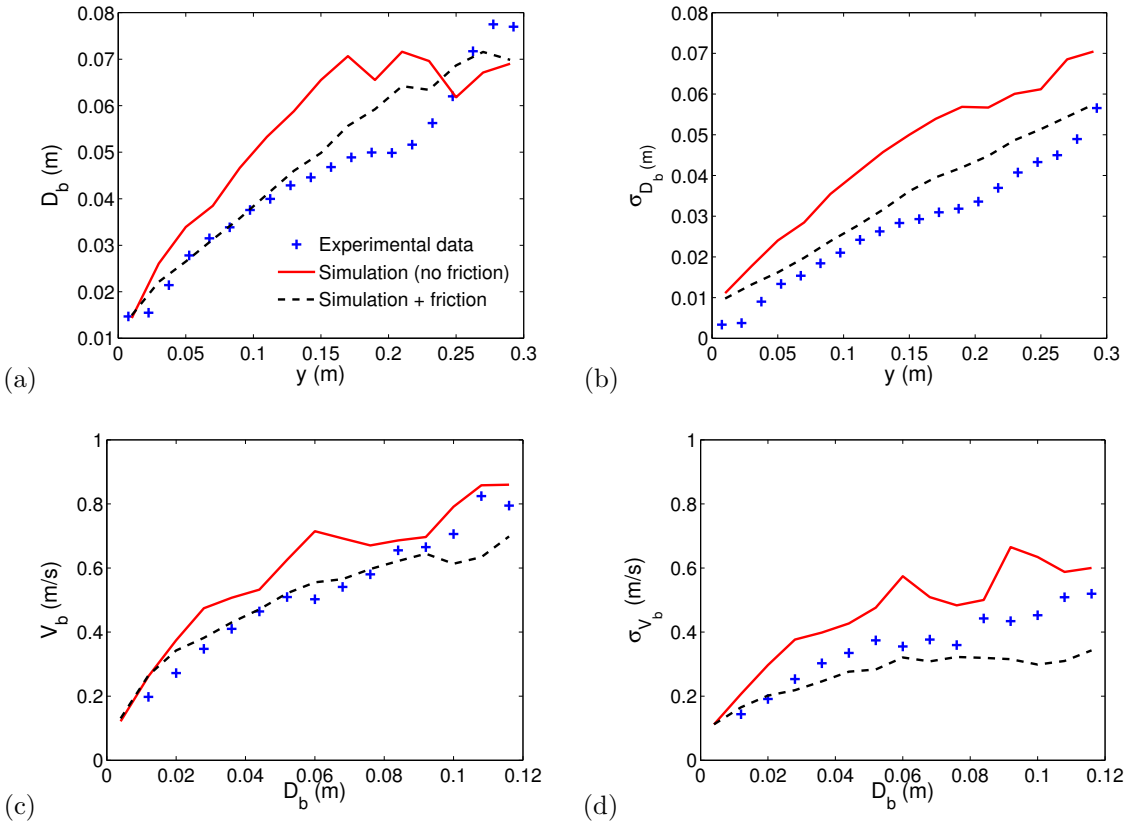

Figure 4: Mean bubble diameter versus vertical distance to the distributor (a) and standard deviation of bubble diameter (b). Mean bubble vertical velocity versus bubble diameter (c) and standard deviation of bubble velocity (d). Experimental and numerical results. Configuration 1.

Figure 5 shows the time-averaged solids velocity vectors, $\vec{V}$, of the PIV measurements reported in [28] (Figure 5a) and the simulation results with the wall−friction term (Figure 5b). The solids concentration map is not included as in Figure 1 because these data are not available for the experimental results. What can be observed from Frigure 5 is a clear preferential path of bubbles towards the centre of the bed with a downflow of particles close to the lateral walls, which is almost identical in the experiment and the simulation with the wall-friction term. The centres of the recirculation of solids in the simulations are placed in similar positions to the recirculations observed in the experiment. The resemblance of these vector maps is more than remarkable considering that the wall-friction term implemented was developed for a bed of different characteristics working under different conditions.

Figure 6 shows the time-averaged vertical solids velocity, V_y, versus the horizontal coordinate, x, at two different distances to the distributir, y, for the experimental results. Figure 6 includes also results of the two-fluid model simulations with the wall-friction term and the simulation with the model proposed by Li and Zhang [21]. The profiles of vertical solids velocity in the 2D simulation calculated with the

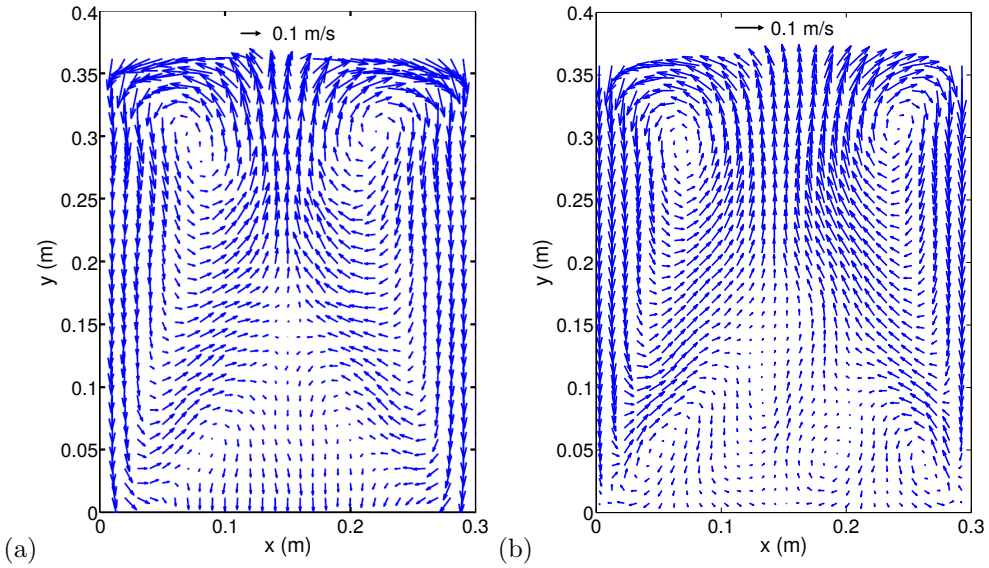

(a) (b)

Figure 5: Time-averaged solids velocity vectors: a) experimental results (adapted from [28]) and b) simulations results with the wall-friction term. Configuration 2.

incorporation of the wall−friction term (Equation 15) are reasonably similar (i.e. shape and magnitude) to the experimental results. This similitude is remarkable since, as commented before, the coefficient of friction used has not been tuned for Configuration 2. The biggest discrepancies appear for the curves at height y = 0.1 m, where the ascending flow, in both the experiment and simulations, is not completely symmetric, indicating that the solids flow seems to be not completely developed at that height, as also commented for the results of Configuration 1. In view of the symmetry of the simulation curves in Figure 6b, the simulated time used to construct the time-averaged data of Configuration 2 seems satisfactory at height y = 0.25 m. Paying further attention to the curve at y = 0.25 m in Figure 6b, the numerical prediction of the velocity profile shape and magnitude using the wall−friction term is considerably good, even in the descending solids region close to the lateral walls where the solids velocity gradients in a pseudo−2D bed tend to be more pronounced. The experimental distributor used by Laverman et al. [28] was a porous plate, which is more alike to the uniform inlet velocity condition set at the distributor in the simulation. This may explain the fine similitude between the experimental and simulation profiles in the region close to the lateral walls in Figure 6b. Especially noticeable is the resemblance of the results obtained with the wall−friction model developed in this work (Equation 15) and the results calculated with the model proposed by Li and Zhang [21], both in shape of the profile and magnitude. This fact confirms the reliability of both models even though considering that they have been developed from different considerations.

Besides, bubble characteristics are also analysed for the present case. Figure 7a shows the bubble diameter, D_b, versus the distance to the distributor, y. Figure 7b represents the bubble velocity, V_b, versus

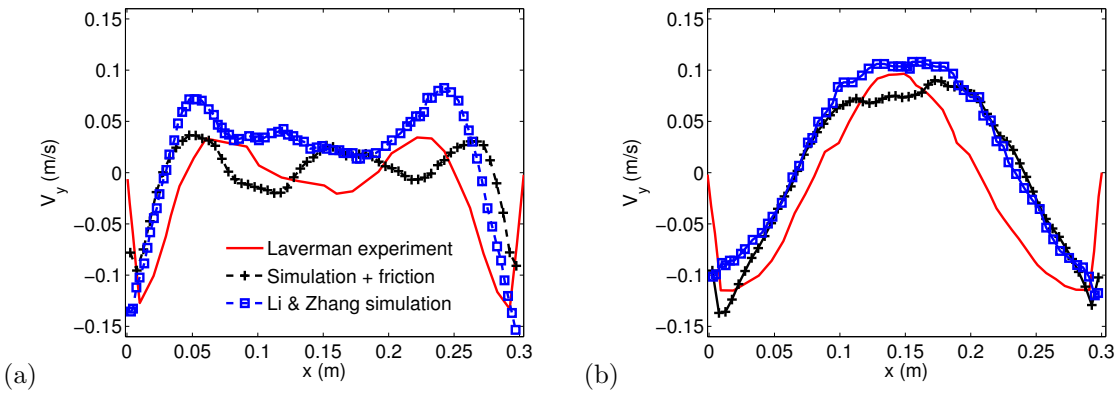

Figure 6: Time-averaged vertical solids velocity versus the horizontal coordinate, x, for the experimental results, the numerical prediction with the wall-friction term and the simulation using the model proposed by Li and Zhang [21]. Results are presented at two distances to the distributor: a) $y = 0.1$ m, and b) $y = 0.25$ m. Configuration 2.

their diameter, D_b. The results correspond to the experimental data reported by Laverman et al. [28] and the 2D simulation with the wall−friction term (Equation 15). The simulation results also include their standard deviation represented with errorbars in Figure 7. Bubbles in the simulation results are identified using the same value of the threshold of solids volume fraction employed in Configuration 1. Figure 7a shows that the numerical results tend to overestimate the mean values of the bubble diameter. This can be attributed to the different threshold technique applied to identify bubbles in [28], where an average image intensity factor was employed to improve illumination in the experimental images. This might introduce differences in bubble detection compared to the threshold technique applied for Configuration 1, whereas the same threshold for the solids volume fraction is employed for the simulations of Configurations 1 and 2. Nevertheless, the difference between the experimental and simulated mean diameter is less than one standard deviation of the data. It is plausible that the differences in the mean bubble diameter seen in Figure 7a lead to the differences observed in the dependence of mean bubble velocity with mean bubble size observed in Figure 7b. In this figure, the experimental mean bubble velocity grows slower than in the simulations. In any case, as for the case of the mean bubble diameter, the experimental mean velocity of bubbles is closer than one standard deviation to the mean bubble velocity obtained with the simulation.

5. Conclusions

A wall−friction model for pseudo−2D bubbling fluidized beds was developed based on experimental results combined with simplifications of the shear force on a wall provided by the theory of granular flows. The model directly introduces the dependence of the wall-friction in pseudo-2D beds on the particle diameter and bed thickness. This allows to simulate pseudo−2D beds using a 2D domain instead of more computationally demanding 3D domain. Two different pseudo-2D fluidized beds were simulated in order to check

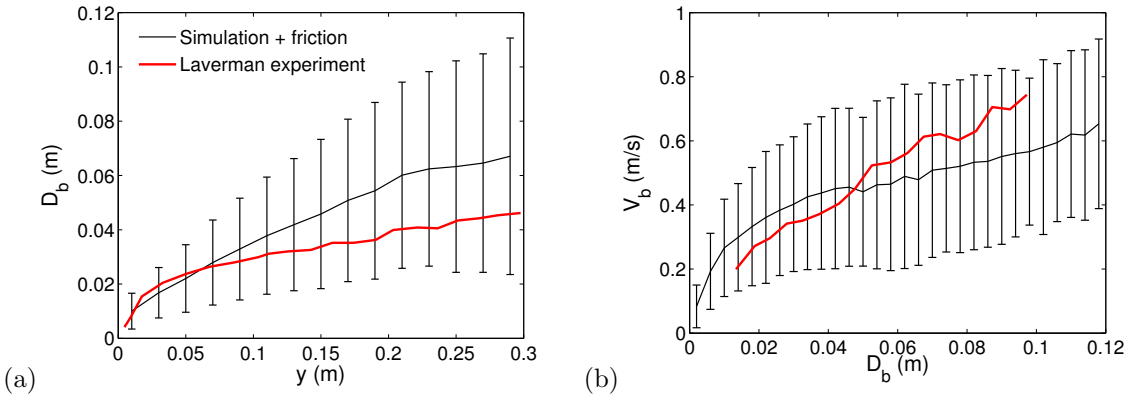

Figure 7: Experimental and numerical results for (a) the bubble diameter versus vertical distance to the distributor and (b) bubble velocity versus bubble diameter. The simulation results also include their standard deviation as errorbars. Configuration 2.

the reliability of the simulation results with the wall−friction term. The simulations results were compared with experimental data concerning important aspects in the fluidized bed dynamics such as solids concentration maps, time-averaged solids vertical velocity and bubble characteristics. The simulation results of both pseudo-2D beds showed that the incorporation of the wall−friction term clearly improves the prediction of the bed behaviour compared to a standard 2D two−fluid model simulations. Results are also consistent with the simulation model proposed by Li and Zhang [21]. Overall, the proposed wall-friction model stands out for its simplicity without compromising numerical convergence, as the model only introduces a linear function of the slip velocity and avoids the incorporation of complex functions of variables, such as the granular temperature, that would affect numerical convergence.

Nomenclature

A_{loc} = local surface area (m^2)

A_L = lateral area (m^2)

A_T = cross−sectional area (m^2)

B = bubble phase probability (−)

C = dense phase probability (−)

c = particle-wall interaction coefficient (kg/m^2s)

D_b = bubble diameter (m)

D_h = hydraulic diameter (m)

d_s = particle diameter (mm)

e_s = particle restitution coefficient (−)

$\vec{F}_{fric,front}$ = local frictional of the front wall (N)

$\vec{F}_{fric,back}$ = local frictional of the back wall (N)

f = friction coefficient for liquids (-)

$\vec{f}_{fric}$ = frictional force per unit volume (N/m^3)

$\vec{g}$ = gravity (m/s^2)

g_0 = the radial distribution function at contact ($-$)

H = bed height (m)

h_0 = static bed height (m)

$\overline{\overline{I}}$ = unity matrix ($-$)

K_{gs} = drag force between gas and solids (kg/(m^{3}s))

k_Θ = diffusion coefficient for granular energy (kg/(ms))

L = duct length (m)

N_f = normal contribution to the shear stress (N)

$\vec{n}$ = unit normal (-)

ΔP = pressure drop(Pa)

p = gas pressure (Pa)

p_s = solids pressure (Pa)

Re = Reynolds number ($-$)

t = time (s)

U = superficial gas velocity (m/s)

U_{mf} = minimum fluidization velocity (m/s)

$\vec{v_g}$ = gas velocity in each computational cell of the TFM (m/s)

$\vec{v_s}$ = bulk solids velocity in each computational cell of the TFM (m/s)

$\vec{v}_{sl}$ = the slip velocity between the particles and the plate (m/s)

v = liquid velocity (m/s)

$\vec{V}$ = velocity vectors (m/s)

V_b = bubble vertical velocity (m/s)

V_y = time-averaged solids vertical velocity (m/s)

x = horizontal coordinate (m)

y = vertical coordinate (m)

y_{cm} = vertical position of the centre of mass of the bed (m)

W = bed width (m)

Z = bed thickness (m)

Greek letters

α_g = gas volume fraction $(-)$

α_s = solids volume fraction $(-)$

$\alpha_{s,max}$ = the solids concentration at closest random packing $(-)$

$\alpha_{s,th}$ = threshold in the solids volume fraction for the bubble detection $(-)$

γ_Θ = collisional dissipation of Θ $(\mathrm{m}^2/\mathrm{s}^2)$

μ = Coulomb coefficient of friction $(-)$

μ_g = gas viscosity (Pa s)

μ_s = solids viscosity (Pa s)

Φ = specularity coefficient (-)

ϕ = angle of internal friction (deg)

$\overline{\overline{\sigma_c}}$ = collisional-translational contribution to the stress tensor (Pa)

$\overline{\overline{\sigma_f}}$ = frictional contribution to the stress tensor (Pa)

ρ_g = gas density $(\mathrm{kg/m}^3)$

ρ_s = solids density $(\mathrm{kg/m}^3)$

τ_{bc} = bulk shear stress in the direction of the slip velocity (N)

$\overline{\overline{\tau_g}}$ = gas stress tensor (Pa)

$\overline{\overline{\tau_s}}$ = solids stress tensor (Pa)

Θ = granular temperature $(\mathrm{m}^2/\mathrm{s}^2)$

Acknowledgments

This work has been partially funded by the Spanish Government (Project DPI2009-10518) and the Autonomous Community of Madrid (Project S2009/ENE-1660).

References

[1] D. Kunii, O. Levenspiel, Fluidization Engineering, 2nd ed., Butterworth-Heinemann, Boston, 1991.

[2] C. M. Boyce, J. F. Davidson, D. J. Holland, S. A. Scott, J. S. Dennis, The origin of pressure oscillations in slugging fluidized beds: Comparison of experimental results from magnetic resonance imaging with a discrete element model, Chemical Engineering Science 116 (2014) 611 – 622.

[3] Y. Chen, J. R. Third, C. R. Müller, A drag force correlation for approximately cubic particles constructed from identical spheres, Chemical Engineering Science 123 (2015) 146 – 154.

[4] E. Cano-Pleite, F. Hernández-Jiménez, A. Acosta-Iborra, Compressible-gas two-fluid modeling of isolated bubbles in a vertically vibrated fluidized bed and comparison with experiments, Chemical Engineering Journal 271 (2015) 287 – 299.

[5] F. Hernández-Jiménez, A. Gómez-García, D. Santana, A. Acosta-Iborra, Gas interchange between bubble and emulsion phases in a 2d fluidized bed as revealed by two-fluid model simulations, Chemical Engineering Journal 215–216 (2013) 479 – 490.

[6] S. Maurer, T. J. Schildhauer, J. R. van Ommen, S. M. Biollaz, A. Wokaun, Scale-up of fluidized beds with vertical internals: Studying the sectoral approach by means of optical probes, Chemical Engineering Journal 252 (2014) 131 – 140.

[7] C. R. Müller, D. J. Holland, J. R. Third, A. J. Sederman, J. S. Dennis, L. F. Gladden, Multi-scale magnetic resonance measurements and validation of discrete element model simulations, Particuology 9 (2011) 330 – 341.

[8] J. van Ommen, J. Valverde, R. Pfeffer, Fluidization of nanopowders: a review, Journal of Nanoparticle Research 14 (2012).

[9] L. Zhou, H. Wang, T. Zhou, K. Li, H. Kage, Y. Mawatari, Model of estimating nano-particle agglomerate sizes in a vibro-fluidized bed, Advanced Powder Technology 24 (2013) 311 – 316.

[10] J. A. M. Kuipers, K. J. Van Duin, F. P. H. Van Beckum, W. P. M. Van Swaaij, A numerical model of gas-fluidized beds, Chemical Engineering Science 47 (1992) 1913 – 1924.

[11] D. Gidaspow, Multiphase flow and Fluidization: Continuum and kinetic theory descriptions, Academic Press, San Diego, CA, 1994.

[12] B. G. M. van Wachem, A. E. Almstedt, Methods for multiphase computational fluid dynamics, Chemical Engineering Journal 96 (2003) 81 – 98.

[13] N. G. Deen, M. Van Sint Annaland, M. A. Van der Hoef, J. A. M. Kuipers, Review of discrete particle modeling of fluidized beds, Chemical Engineering Science 62 (2007) 28 – 44.

[14] C. R. Müller, D. J. Holland, A. J. Sederman, S. A. Scott, J. S. Dennis, L. F. Gladden, Granular temperature: Comparison of magnetic resonance measurements with discrete element model simulations, Powder Technology 184 (2008) 241 – 253.

[15] F. Hernández-Jiménez, L. M. García-Gutiérrez, A. Soria-Verdugo, A. Acosta-Iborra, Fully coupled TFM-DEM simulations to study the motion of fuel particles in a fluidized bed, Chemical Engineering Science 134 (2015) 57 – 66.

[16] J. R. Grace, F. Taghipour, Verification and validation of CFD models and dynamic similarity for fluidized beds, Powder Technology 139 (2004) 99 – 110.

[17] J. R. Grace, T. Li, Complementarity of CFD, experimentation and reactor models for solving challenging fluidization problems, Particuology 8 (2010) 498 – 500.

[18] N. G. Deen, S. H. Kriebitzsch, M. A. van der Hoef, J. Kuipers, Direct numerical simulation of flow and heat transfer in dense fluid–particle systems, Chemical Engineering Science 81 (2012) 329 – 344.

[19] N. G. Deen, E. Peters, J. T. Padding, J. Kuipers, Review of direct numerical simulation of fluid–particle mass, momentum and heat transfer in dense gas–solid flows, Chemical Engineering Science 116 (2014) 710 – 724.

[20] F. Hernández-Jiménez, J. Sánchez-Prieto, A. Soria-Verdugo, A. Acosta-Iborra, Experimental quantification of the particle-wall frictional forces in pseudo-2D gas fluidised beds, Chemical Engineering Science 102 (2013) 257 – 267.

[21] T. Li, Y. Zhang, A new model for two-dimensional numerical simulation of pseudo-2D gas-solids fluidized beds, Chemical Engineering Science 102 (2013) 246 – 256.

[22] T. Li, J. R. Grace, X. Bi, Study of wall boundary condition in numerical simulations of bubbling fluidized beds, Powder Technology 203 (2010) 447 – 457.

[23] F. Hernández-Jiménez, S. Sánchez-Delgado, A. Gómez-García, A. Acosta-Iborra, Comparison between two-fluid model simulations and particle image analysis & velocimetry (PIV) results for a two-dimensional gas-solid fluidized bed, Chemical Engineering Science 66 (2011) 3753 – 3772.

[24] T. Kawaguchi, T. Tanaka, Y. Tsuji, Numerical simulation of two-dimensional fluidized beds using the discrete element method (comparison between the two- and three-dimensional models), Powder Technology 96 (1998) 129 – 138.

[25] Y. Q. Feng, A. B. Yu, Effect of bed thickness on the segregation behavior of particle mixtures in a gas fluidized bed, Industrial & Engineering Chemistry Research 49 (2010) 3459 – 3468.

[26] T. Li, P. Gopalakrishnan, R. Garg, M. Shahnam, CFD-DEM study of effect of bed thickness for bubbling fluidized beds,

Particuology 10 (2012) 532 – 541.

[27] F. Hernández-Jiménez, T. Li, E. Cano-Pleite, W. Rogers, A. Acosta-Iborra, Characterization of the particle-wall frictional forces in pseudo-2D fluidized beds using DEM, Chemical Engineering Science 116 (2014) 136 – 143.

[28] J. A. Laverman, I. Roghair, M. van Sint Annaland, H. Kuipers, Investigation into the hydrodynamics of gas-solid fluidized beds using particle image velocimetry coupled with digital image analysis, Canadian Journal of Chemical Engineering 86 (2008) 523 – 535.

[29] P. C. Johnson, R. Jackson, Frictional-collisional constitutive relations for granular materials, with application to plane shearing, Journal of Fluid Mechanics 176 (1987) 67 – 93.

[30] M. Syamlal, W. Rogers, T. J. O'Brien, MFIX Documentation: Theory Guide, U.S. Department of Energy (DOE), Morgantown Energy Technology Center, Morgantown, West Virginia, 1993.

[31] S. Benyahia, M. Syamlal, T. J. O'Brien, Summary of MFIX equations 2005-4, 2007.

[32] J. K. Sveen, Matpiv, 1998 - 2007. URL: `http://www.math.uio.no/jks/matpiv/`.

[33] N. Otsu, Threshold selection method from gray-level histograms., IEEE Trans Syst Man Cybern SMC-9 (1979) 62–66.